PCH_2, $^2J(AB)$ = 13.8 Hz, $^2J(AX)$ = 4.7 Hz, $^2J(BX)$ = 14 Hz), 5.51 (dd, 1 H, PCH, $J(PH)$ = 1.1, 7.3 Hz), 7.18-8.78 (aromatic H), N*H* resonance not assigned. $^{31}P\{^1H\}$ NMR (CD_2Cl_2): δ 4.2 (s, Ph_2PC), 135.2 (s, PO). $^{13}C\{^1H\}$ NMR (CD_2Cl_2): δ 34.53 (d, PCH_2, $J(PC)$ = 31.6 Hz), 91.30 (d, PCH, $J(PC)$ = 64.5 Hz), 163.71 (s, CO).

***cis*-[Pd{Ph_2PCH=C(O)Ph}{PhP(O)(o-$C_6H_4CH_2NMe_2$)}] (11).** A 10-fold excess of Na_2CO_3 was added to a solution of **9** (0.210 g, 0.25 mmol) in undried CH_2Cl_2 (40 mL), and the reaction mixture was stirred for 8 h. The suspended Na_2CO_3 was filtered off, and the solution was concentrated under reduced pressure. Addition of pentane afforded yellow crystals of **11** (yield 0.145 g, 87%; mp 205 °C dec). Anal. Calcd for $C_{35}H_{33}NO_2P_2Pd$ (M_r = 668.0): C, 62.93; H, 4.98. Found: C, 62.30; H, 4.95. IR (KBr): 1581 w, 1509 s, 1480 s cm^{-1}. ^1H NMR (C_6D_6): δ 2.04 (δ_A) and 2.98 (δ_B) (ABXY spin system (with X, Y = P), 2 H, NCH_2, $^2J(AB)$ = 12.3 Hz, $^4J(AX)$ = $^4J(AY) \approx 0$ Hz, $^4J(BX)$ = 4.1 Hz, $^4J(BY)$ = 7.2 Hz), 2.20 (d, 3 H, CH_3, $^4J(PH) < 0.5$ Hz), 2.43 (d, 3 H, CH_3, $^4J(PH) < 0.5$ Hz), 4.90 (dd, 1 H, PCH, $J(PH)$ = 3.0, 2.0 Hz), 6.52-9.23 (24 H, aromatic H). $^{31}P\{^1H\}$ NMR ($CDCl_3$): δ 32.3 (s, Ph_2PC), 61.1 (s, PO).

***cis*-[Pd{Ph_2PCH=C(O)Ph}{PhP(O)$CH_2C_9H_6N$}] (12).** This complex was prepared by starting from **10** (0.192 g, 0.25 mmol), with use of the procedure described for **11**. Addition of pentane afforded yellow crystals of **12** (yield 0.157 g, 79%; mp 180 °C dec). Crystals suitable for X-ray analysis were obtained by slow diffusion of pentane into a $CHCl_3$ solution of **12**. Anal. Calcd for $C_{36}H_{29}NO_2P_2Pd \cdot CHCl_3$ (M_r = 795.4): C, 55.88; H, 3.80. Found: C, 54.53; H, 3.90. IR (KBr): 1581 w, 1513 s, 1480 s cm^{-1}. ^1H NMR (CD_2Cl_2): δ 3.49 (δ_A) and 4.16 (δ_B) (ABX spin system (with X = *P*(O)), 2 H, PCH_2, $^2J(AB) = {}^2J(AX) = {}^2J(BX)$ = 14.7 Hz), 4.84 (dd, 1 H, PCH, $J(PH)$ = 3.7, 1.7 Hz), 6.82-10.39 (26 H, aromatic H). $^{31}P\{^1H\}$ NMR (CD_2Cl_2): δ 30.0 (s, Ph_2PC), 70.2 (s, PO).

Crystal Structure Determination of 12. Crystals of **12**·$CHCl_3$ have a parallelepipedic habit and were obtained by slow cooling of a concentrated $CHCl_3$ solution of **12**. Pertinent crystal data are presented in Table II. Precise lattice parameters were determined by standard Enraf-Nonius least-squares methods using 25 carefully selected reflections. Intensity data were collected on an automatic four-circle diffractometer. No intensity decay was observed during the data collection period. For all subsequent computations the Enraf-Nonius SDP package was used.[20] Intensities were corrected for Lorentz/polarization factors. Absorption corrections were omitted in view of the low linear absorption coefficient. The crystal structure was solved by using Patterson and Fourier methods[21] and refined by full-matrix least-squares with anisotropic thermal parameters for all non-hydrogen atoms. The function minimized was $\sum w(|F_o| - |F_c|)^2$, where the weight is $4I/[\sigma^2(I) + (0.04I)^2]$. Hydrogen atoms were introduced by their computed coordinates (C-H distance 0.95 Å) in structure factor calculations and were assigned isotropic thermal parameters of B = 5.0 Å^2 except for H(1A), which was positioned by Fourier difference but not refined. The final difference map showed no significant residual peaks. The neutral-atom scattering factors used for all atoms and anomalous scattering factors for all non-hydrogen atoms were obtained from standard sources.[22] Atomic coordinates with estimated standard deviations corresponding to the final least-squares refinement cycles are given in Table III. Refinement results are given in Tables I and S-I (supplementary material). Hydrogen atom coordinates (Table S-II), anisotropic thermal parameters for all non-hydrogen atoms (Table S-III), all bond distances and angles (Table S-IV), and the observed and calculated structure factor amplitudes used in the refinement (Tables S-VI) are available as supplementary material.[14]

Acknowledgment. We thank A. Degremont for the preparation of $Ph_2PCH_2C(O)Ph$ and Dr. M. Pfeffer for helpful discussion. This work was supported by the CNRS and the GS CO_2.

Supplementary Material Available: Crystallographic data (Table S-I), hydrogen atom coordinates (Table S-II), anisotropic thermal parameters (Table S-III), all bond distances and angles (Table S-IV), and selected least-squares planes (Table S-V) (11 pages); observed and calculated structure factors (Table S-VI) (14 pages). Ordering information is given on any current masthead page.

(20) Frenz, B. A. In *Computing in Crystallography*; Schenk, H., Olthof-Hazekamp, R., van Koningsveld, H., Bassi, G. C., Eds.; Delft University Press: Delft, The Netherlands, 1978; pp 64-71.
(21) Germain, G.; Main, P.; Woolfson, M. M. *Acta Crystallogr., Sect. A: Cryst. Phys., Diffr., Theor. Gen. Crystallogr.* **1971**, *A27*, 368-376.
(22) *International Tables for X-ray Crystallography*; Kynoch: Birmingham, England, 1974; Vol. IV, p 99.

Contribution from the Department of Chemistry, University Center at Binghamton, State University of New York, Binghamton, New York 13901

Solvent Effects on the Lowest Energy Excited States of Binuclear $(OC)_5W$-L-$W(CO)_5$ Complexes

Mthembeni M. Zulu and Alistair J. Lees*

Received January 5, 1988

Electronic absorption, emission, photochemical, and redox potential data have been obtained for mononuclear $(OC)_5WL$ and binuclear $(OC)_5W$-L-$W(CO)_5$ complexes, where L = pyrazine (pyz), 4,4′-bipyridine (bpy), and 1,2-bis(4-pyridyl)ethane (bpa), in various solvents. Low-lying $^1A_1 \rightarrow {}^1E$ ligand-field (LF) and $W(d\pi) \rightarrow \pi^*(L)$ charge-transfer (MLCT) transitions are observed for each complex; the MLCT absorption bands exhibit a strong negative solvatochromism. In very nonpolar solvents the MLCT band envelope indicates the presence of two components, assigned to orbitally allowed *y*- and *z*-polarized MLCT transitions. The energy positions of the MLCT transitions depend substantially on the nature of L; when L = bpa, the LF states are at lowest energy, but when L = pyz and bpy, the MLCT states are lowest lying. Changes in metal-ligand bond polarity between the ground and excited states and specific solvent-solute and induced dipolar interactions contribute to the MLCT solvatochromism; these effects are correlated with the electronic characteristics of L and the nature of the MLCT transition. Emission has been recorded from the pyz and bpy complexes at 283 K, in accordance with the MLCT assignment. Dual MLCT emission bands have been observed, but lifetime data reveal that these MLCT states are thermally equilibrated. Emission spectra exhibit solvent shifts in the direction opposite to that for absorption spectra, and this effect is rationalized on the basis of a scheme that depicts a contraction of the W-N bond in the excited state relative to the ground-state geometry. Solvent predominantly affects the nonradiative decay rates; in some cases k_{nr} data illustrate an energy gap law dependence, but specific solute-solvent and induced dipolar interactions are also deemed important. Solvent effects on redox potential data substantiate the HOMO/LUMO assignments and further indicate the extent of Franck-Condon perturbation. On photolysis the complexes undergo W-N bond dissociation; effects of solvent on this reaction efficiency are small and are incorporated in the excited-state model.

Introduction

Currently, there is substantial interest in metal complexes that are bridged through ligands containing a delocalized π system. In particular, such ligand-bridged dimer complexes have been studied as models for inner-sphere electron-transfer processes between metal centers,[1] and they have received attention because

0020-1669/88/1327-3325$01.50/0

of their relevance to low-dimensional conducting coordination polymers[2] and metalloenzyme systems.[3]

A number of spectroscopic, photochemical, and electrochemical studies have been carried out on ligand-bridged metal carbonyl complexes, and these have demonstrated that the binucleating ligand π^* system may be perturbed greatly from that of the corresponding mononuclear species.[4] Recently, we reported pronounced effects on the electronic absorption, redox, photophysical, and photochemical properties of a series of homonuclear and heteronuclear $(OC)_5M-L-M'(CO)_5$ (M, M' = Cr, Mo, W) complexes through variations in the electronic stabilization of the bridging ligand π^* system.[5] Although there has been much interest recently in the effects of solvent on the absorption spectra of organometallic complexes,[6] relatively few complete studies of luminescence, photochemical, and redox properties have appeared.[7] Much remains to be understood about the role of solvent in optical and photochemical processes of metal complexes.

This paper concerns the effects of solvent on the lowest energy excited states and excited-state properties of ligand-bridged $(OC)_5W-L-W(CO)_5$ complexes. These binuclear $(OC)_5W-L-W(CO)_5$ complexes are ideal for this type of investigation, as they are known to exhibit intense and extremely solvent-sensitive metal to ligand charge-transfer (MLCT) absorption bands, and from a practical sense they are soluble and thermally stable in a wide range of organic media.[6k] Indeed, the MLCT band of the $(OC)_5W(pyz)W(CO)_5$ complex exhibits a remarkable solvent dependence, blue-shifting up to 5800 cm^{-1} as the solution becomes more polar.[4f,6l] In this particular compound the low-lying MLCT states are so intense and well separated from higher energy ligand field levels that it is possible to study directly the effects of varying solvent on their spectroscopic and photochemical properties. Moreover, a number of these ligand-bridged binuclear $(OC)_5W-L-W(CO)_5$ complexes have recently been observed to be luminescent in fluid solution,[5] and this provides an excellent opportunity to probe the solvent dependence of the excited-state energy levels and deactivation processes in these molecules. In this article we report solvent effects on the electronic absorption, photophysical, photochemical, and redox properties of a series of binuclear $(OC)_5W-L-W(CO)_5$ complexes. The binucleating ligands (L) employed here are pyrazine (pyz), 4,4'-bipyridine (bpy), and 1,2-bis(4-pyridyl)ethane (bpa). A comparison is also made with the corresponding mononuclear $(OC)_5WL$ derivatives.

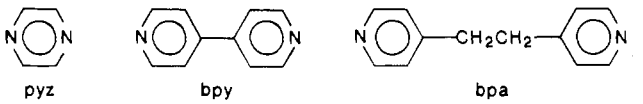

Experimental Section

Materials. Tungsten hexacarbonyl was obtained from Strem Chemical Co. and used without further purification. The ligands pyz, bpy, and bpa were purchased from Aldrich Chemical Co. and recrystallized prior to use. Tetrahydrofuran (THF) used in synthetic procedures was distilled from $LiAlH_4$ and stored under an argon atmosphere. Solvents used in the spectroscopic experiments were obtained from J. T. Baker Chemical Co. as HPLC or Photrex grade. Methylene chloride and *N,N'*-dimethylformamide used in the electrochemical measurements were of HPLC grade that had been dried over 4-Å molecular sieves and distilled before use. Tetrabutylammonium perchlorate (TBAP) used as supporting electrolyte was rigorously dried (in vacuo at 60 °C for 12 h) prior to use. Nitrogen used for the purging experiments was dried and deoxygenated according to a previously reported method.[8] Other chemicals and solvents used were of the best commercial grade. The complexes were purified by chromatography on 80–200-mesh alumina that had been obtained from Fisher Scientific Co.

Syntheses. The mononuclear $(OC)_5WL$ and binuclear $(OC)_5W-L-W(CO)_5$ (L = pyz, bpy, bpa) complexes were prepared and characterized as described previously.[5] These compounds are stable as solids for long periods if kept in the dark under N_2.

Equipment and Procedures. Electronic absorption spectra were obtained on a Hewlett-Packard 8450A spectrometer, which incorporates a microprocessor-controlled diode-array detector. This enabled absorption spectra to be obtained within 5 s of complex dissolution, if required. Reported absorption maxima are accurate to ±2 nm. Emission and excitation spectra were recorded on a SLM Instruments Model 8000/8000S spectrometer, which utilizes a photomultiplier-based photon-counting detector. These spectra were fully corrected for variations in the detector response and excitation lamp intensity as a function of wavelength; obtained band maxima are accurate to within ±4 nm. In the emission and excitation experiments the sample solutions were filtered through 0.22-μm Millipore filters and deoxygenated prior to taking measurements; the solution temperature was controlled to ±0.1 K.

Emission lifetimes (τ_e) were obtained on a PRA System 3000 time-correlated pulsed single-photon-counting apparatus.[9] Samples were excited at 400 nm with light from a PRA Model 510 nitrogen flash lamp that had been transmitted through an Instruments SA Inc. H-10 monochromator. Emission was detected from the sample at 90° by means of a second H-10 monochromator and a thermoelectrically cooled red-sensitive Hamamatsu R955 photomultiplier tube; the photon counts were stored on a Tracor Northern Model 7200 microprocessor-based multichannel analyzer. The instrument response function was then deconvoluted from the emission data to obtain an undisturbed decay that was then fitted by a least-squares method on an IBM PC. Each sample gave rise to single-exponential decays; the lifetimes were reproducible to within ±5 ns. Emission quantum yields (ϕ_{em}) were determined with dilute $Ru(bpy)_3^{2+}$ in deoxygenated aqueous solution at 283 K as a calibrant ($\phi_{em} = 0.046$)[10] and were corrected for differing refractive indices of the solvents;[11] the emission quantum yields are accurate to ±10%. Radiative (k_r) and nonradiative (k_{nr}) decay rate constants were obtained from the emission lifetimes (τ_e) and quantum yield (ϕ_{em}) data, according to eq 1 and 2. In the application of eq 1, it is assumed that the emissive state

$$\phi_{em} = k_r\tau_e \quad (1)$$

$$\tau_e = (k_r + k_{nr})^{-1} \quad (2)$$

is formed with unit efficiency, as recognized for several other substituted metal carbonyl systems.[7]

(1) (a) Creutz, C.; Taube, H. *J. Am. Chem. Soc.* **1969**, *91*, 3988; **1973**, *95*, 1086. (b) Fürholz, U.; Burgi, H.-B.; Wagner, F. E.; Stebler, A.; Ammeter, J. H.; Krausz, E.; Clark, R. J. H.; Stead, M. J.; Ludi, A. *J. Am. Chem. Soc.* **1984**, *106*, 121. (c) Haim, A. *Acc. Chem. Res.* **1975**, *8*, 264. (d) Cannon, R. D. *Electron Transfer Reactions*; Butterworths: London, 1980.
(2) Hoffman, B. M.; Ibers, J. A. *Acc. Chem. Res.* **1983**, *16*, 15.
(3) (a) Spiro, T. G., Ed. *Copper Proteins*; Wiley-Interscience: New York, 1981. (b) Bencini, A.; Benelli, C.; Gatteschi, D.; Zanchini, C. *Inorg. Chem.* **1986**, *25*, 398. (c) Morganstern-Badarau, I.; Cocco, D.; Desideri, A.; Rotilio, G.; Jordanov, J.; Dupre, N. *J. Am. Chem. Soc.* **1986**, *108*, 300.
(4) (a) Pannell, K. H.; Guadalupe de la Paz Saenz Gonzalez, M.; Leano, H.; Iglesias, R. *Inorg. Chem.* **1978**, *17*, 1093. (b) Pannell, K. H.; Iglesias, R. *Inorg. Chim. Acta* **1979**, *33*, L161. (c) Daamen, H.; Stufkens, D. J.; Oskam, A. *Inorg. Chim. Acta* **1980**, *39*, 75. (d) Gaus, P. L.; Boncella, J. M.; Rosengren, K. S.; Funk, M. O. *Inorg. Chem.* **1982**, *21*, 2174. (e) Garber, L. L. *Inorg. Chem.* **1982**, *21*, 3244. (f) Lees, A. J.; Fobare, J. M.; Mattimore, E. F. *Inorg. Chem.* **1984**, *23*, 2709. (g) Ernst, S.; Kaim, W. *Angew. Chem., Int. Ed. Engl.* **1985**, *24*, 430. (h) Kohlmann, S.; Ernst, S.; Kaim, W. *Angew. Chem., Int. Ed. Engl.* **1985**, *24*, 684. (i) Kaim, W.; Kohlmann, S. *Inorg. Chim. Acta* **1985**, *101*, L21. (j) Haga, M.-A.; Koizumi, K. *Inorg. Chim. Acta* **1985**, *104*, 47. (k) Ernst, S.; Kaim, W. *J. Am. Chem. Soc.* **1986**, *108*, 3578. (l) Gross, R.; Kaim, W. *Inorg. Chem.* **1986**, *25*, 498. (m) Kaim, W.; Kohlmann, S. *Inorg. Chem.* **1987**, *26*, 68.
(5) Zulu, M. M.; Lees, A. J. *Inorg. Chem.* **1988**, *27*, 1139.
(6) (a) Bock, H.; tom Dieck, H. *Angew. Chem., Int. Ed. Engl.* **1966**, *5*, 520. (b) Saito, H.; Fujita, J.; Saito, K. *Bull. Chem. Soc. Jpn.* **1968**, *41*, 863. (c) Burgess, J. *J. Organomet. Chem.* **1969**, *19*, 218. (d) tom Dieck, H.; Renk, I. W. *Angew. Chem., Int. Ed. Engl.* **1970**, *9*, 793. (e) Walther, D. Z. *Anorg. Allg. Chem.* **1973**, *396*, 46. (f) Walther, D. *J. Prakt. Chem.* **1974**, *316*, 604. (g) Wrighton, M. S.; Morse, D. L. *J. Organomet. Chem.* **1975**, *97*, 405. (h) Burgess, J.; Chambers, J. G.; Haines, R. I. *Transition Met. Chem. (Weinheim, Ger.)* **1981**, *6*, 145 and references therein. (i) Manuta, D. M.; Lees, A. J. *Inorg. Chem.* **1983**, *22*, 3825. (j) Connor, J. A.; Overton, C.; El Murr, N. *J. Organomet. Chem.* **1984**, *277*, 277. (k) Dodsworth, E. S.; Lever, A. B. P. *Chem. Phys. Lett.* **1984**, *112*, 567. (l) Manuta, D. M.; Lees, A. J. *Inorg. Chem.* **1986**, *25*, 3212. (m) Kaim, W.; Kohlmann, S. *Inorg. Chem.* **1986**, *25*, 3306. (n) Kaim, W.; Kohlmann, S.; Ernst, S.; Olbrich-Deussner, B.; Bessenbacher, C.; Schulz, A. *J. Organomet. Chem.* **1987**, *321*, 215.
(7) Lees, A. J. *Chem. Rev.* **1987**, *87*, 711.
(8) Schadt, M. J.; Gresalfi, N. J.; Lees, A. J. *Inorg. Chem.* **1985**, *24*, 2942.
(9) O'Connor, D. V.; Phillips, D. *Time-Correlated Single Photon Counting*; Academic: London, 1984.
(10) Van Houten, J.; Watts, R. J. *J. Am. Chem. Soc.* **1976**, *98*, 4853.
(11) Demas, J. N.; Crosby, G. A. *J. Phys. Chem.* **1971**, *75*, 991.

Table I. Electronic Absorption Spectral Data (λ_{max}, nm ($10^{-4}\epsilon$, M^{-1} cm^{-1})) and Assignments for $(OC)_5WL$ and $(OC)_5W-L-W(CO)_5$ Complexes in Various Solvents at 298 K

complex		CH_2Cl_2	$CHCl_3$	C_6H_6	C_7H_{14}/C_6H_6[a]	CCl_4[b]	C_8H_{18}
$(OC)_5W(pyz)W(CO)_5$	LF	395 (0.60)	395 (0.66)	397 (0.55)	396 (0.63)	396 (0.60)	396 (0.56)
	MLCT	521 (1.28)	539 (1.36)	510 (1.20)	534 (1.35)	548 (1.40), 590[c]	552 (1.44), 595[c]
$(OC)_5W(bpy)W(CO)_5$	LF	402 (1.47)	404 (1.06)	404 (1.18)	404 (1.10)	404 (0.80)	404 (0.76)
	MLCT	431 (1.14)	432 (0.94)	438 (1.08)	446 (1.11), 500[c]	452 (1.20), 502[c]	462 (1.23), 504[c]
$(OC)_5W(bpa)W(CO)_5$	LF	379 (1.50)	377 (1.46)	379 (1.22)	379 (1.28)	381 (1.40)	380 (1.45)
	MLCT	335[c]	342 (1.63)	343 (1.29)	349 (1.32)	358[c]	362[c]
$(OC)_5W(pyz)$	LF	397 (0.87)	399 (1.00)	398 (0.71)	402 (0.75)	402 (0.74)	402 (0.70)
	MLCT	*d*	*d*	*d*	*d*	420[c]	424[c]
$(OC)_5W(bpy)$	LF	402 (1.26)	402 (1.15)	400 (1.03)	404 (1.00)	404 (0.90)	404 (0.79)
	MLCT	*d*	*d*	*d*	*d*	*d*	*d*
$(OC)_5W(bpa)$	LF	383 (0.25)	380 (0.27)	379 (0.30)	381 (0.34)	381 (0.37)	381 (0.39)
	MLCT	*d*	*d*	340[c]	342[c]	345[c]	346[c]

[a] 5:1 (v/v). [b] Recorded within 5 s of dissolution to minimize thermal decomposition reaction. [c] Observed as a shoulder. [d] Overlaps with LF transition.

Electrochemical measurements were recorded on a Bio-Analytical Systems Corrosion Model CV-47 voltammograph with a Houston Instruments Model 200 X-Y recorder. Cyclic voltammograms were obtained in deoxygenated dry solvents under a nitrogen atmosphere. A glassy-carbon working electrode, a platinum-wire auxiliary electrode, and a saturated calomel reference electrode (SCE) were used in these experiments with 0.1 M tetrabutylammonium perchlorate (TBAP) as supporting electrolyte. The measurements were calibrated with ferrocene, and the reported values are uncorrected for the liquid-junction potential, which is estimated to be less than 0.01 V. The concentration of the metal carbonyl complexes in these measurements was $\sim 10^{-3}$ M, and the scan rate was 80 mV s^{-1}.

Photolysis experiments at 458 and 514 nm were performed with a Lexel Corp. Model 95-4 4W argon ion laser with a typical laser power of 40 mW. The photon flux was calculated from the laser power, determined by means of an external Lexel Corp. Model 504 power meter. Sample solutions ($\sim 10^{-4}$ M complex and 10^{-2} M entering ligand) were filtered through 0.22-μm Millipore filters immediately before use and deoxygenated prior to photolysis; the solution temperature was controlled to ±0.1 K. In all photolysis experiments the concentrations of reactants and products were followed by UV-vis spectroscopy. Photochemical quantum yields were corrected for inner-filter effects due to product formation and changing degree of light absorption when necessary. Measurements were typically made over relatively small (<20%) conversions, and the quantum yields were found to be reproducible to ±10%.

Results

These ligand-bridged $(OC)_5W-L-W(CO)_5$ complexes are fairly soluble and thermally stable in a wide range of organic media, although in room-temperature solution they are apt to undergo a slow decomposition reaction involving cleavage of the W–N bond, as noted previously for $(OC)_5Mo(pyz)Mo(CO)_5$.[12] This thermal decomposition was typically only troublesome for the mononuclear complexes in polar solvents. The solvents chosen for this study are dimethylformamide, methylene chloride, chloroform, benzene, methylcyclohexane/benzene (5:1 v/v), carbon tetrachloride, and isooctane. Figure 1 illustrates absorption spectra obtained from the series of binuclear $(OC)_5W-L-W(CO)_5$ complexes in benzene and isooctane. A list of the absorption data recorded for all the complexes in the full range of solvents studied is shown in Table I.

Room-temperature luminescence spectra have been observed from solutions of the $(OC)_5WL$ and $(OC)_5W-L-W(CO)_5$ complexes where L = pyz and bpy, but not from the corresponding bpa derivatives. Representative solvent effects on the emission spectra of $(OC)_5W(bpy)W(CO)_5$ are illustrated in Figure 2, and the photophysical parameters measured from all the complexes studied are summarized in Table II. Emission data were not obtained in carbon tetrachloride or isooctane due to limited solubility. The $(OC)_5W-L-W(CO)_5$ (L = pyz, bpy) complexes in C_7H_{14}/C_6H_6 (5:1 v/v) solution noticeably exhibit band structure indicating dual emission features. Importantly, the spectral distribution of all complexes is independent of excitation wavelengths between 300 and 500 nm, and the lifetimes are constant

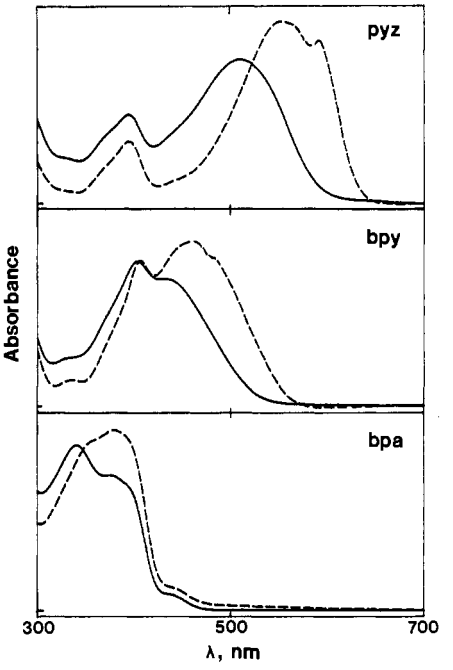

Figure 1. Electronic absorption spectra of $(OC)_5W-L-W(CO)_5$ (L = pyz, bpy, bpa) complexes in (—) benzene and (- - -) isooctane at 298 K.

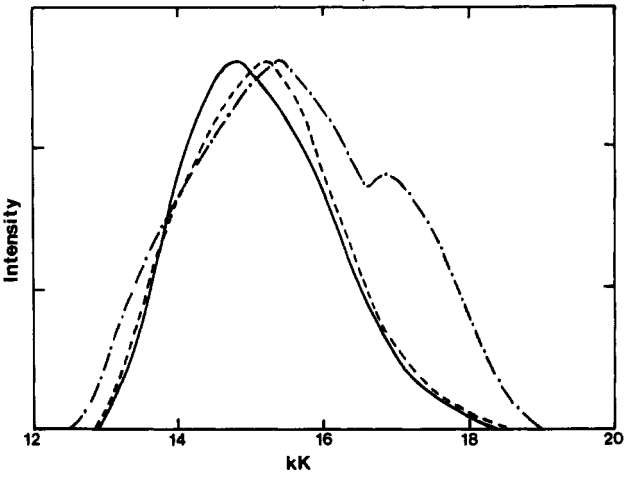

Figure 2. Luminescence spectra of $(OC)_5W(bpy)W(CO)_5$ in deoxygenated solutions of (—) CH_2Cl_2, (- - -) $CHCl_3$, and (-·-) C_7H_{14}/C_6H_6 (5:1 v/v) at 283 K. Emission maxima are normalized.

(and strictly exponential) throughout the emission band. Solvent effects on excitation spectra of the $(OC)_5WL$ and $(OC)_5W-L-W(CO)_5$ complexes are summarized in Table III.

Redox potentials obtained from cyclic voltammetry data of the free ligands and the metal carbonyl complexes in CH_2Cl_2, DMF,

(12) Ernhoffer, R.; Shepherd, R. E. *J. Chem. Soc., Chem. Commun.* **1978**, 859.

Table II. Emission Data and Derived Radiative (k_r) and Nonradiative (k_{nr}) Decay Rate Constants for $(OC)_5WL$ and $(OC)_5W$–L–$W(CO)_5$ Complexes in Various Solvents[a]

complex	solvent	λ_{max}, nm	$10^4\phi_{em}$[b]	τ_e,[c] ns	k_r, $s^{-1} \times 10^2$	k_{nr}, $s^{-1} \times 10^6$
$(OC)_5W(pyz)W(CO)_5$[d]	CH_2Cl_2	730	1.60	103	15.5 ± 2.5	9.7 ± 0.5
	$CHCl_3$	741	2.90	153	19.0 ± 2.5	6.5 ± 0.3
	C_6H_6	721	5.00	206	24.3 ± 3.1	4.9 ± 0.2
	C_7H_{14}/C_6H_6[e]	650,[f] 759	7.00	284	24.6 ± 3.0	3.5 ± 0.1
$(OC)_5W(bpy)W(CO)_5$	CH_2Cl_2	678	0.38	121	3.1 ± 0.5	8.3 ± 0.4
	$CHCl_3$	660	0.95	220	4.3 ± 0.5	4.5 ± 0.2
	C_6H_6	654	1.59	394	4.0 ± 0.5	2.5 ± 0.1
	C_7H_{14}/C_6H_6[e]	595,[f] 649	1.60	429	3.7 ± 0.5	2.3 ± 0.1
$(OC)_5W(bpa)W(CO)_5$		[g]				
$(OC)_5W(pyz)$[d]	CH_2Cl_2	649	0.29	42	7.1 ± 1.2	23.8 ± 1.2
	$CHCl_3$	656	0.39	43	9.1 ± 1.4	23.3 ± 1.1
	C_6H_6	645	0.21	18	11.8 ± 2.5	55.6 ± 7.9
	C_7H_{14}/C_6H_6[e]	639	0.14	12	12.0 ± 3.2	83.3 ± 16.7
$(OC)_5W(bpy)$	CH_2Cl_2	660	0.24	178	1.4 ± 0.2	5.6 ± 0.2
	$CHCl_3$	656	0.56	213	2.6 ± 0.3	4.7 ± 0.1
	C_6H_6	643	0.72	415	1.7 ± 0.2	2.4 ± 0.1
	C_7H_{14}/C_6H_6[e]	640	0.72	399	1.8 ± 0.2	2.5 ± 0.1
$(OC)_5W(bpa)$		[g]				

[a] Observed in 4×10^{-5}–2×10^{-4} M deoxygenated solutions. Spectra corrected for variation in instrumental response as a function of wavelength. All values obtained at 283 K unless otherwise stated. Excitation wavelength is 400 nm. [b] Absolute quantum yields measured relative to the emission of $Ru(bpy)_3^{2+}$; accurate to within ±10%. [c] Lifetimes accurate to within 5 ns, except for $(OC)_5W(pyz)$, where errors are ±2 ns. [d] Data obtained at 298 K. [e] 5:1 (v/v). [f] Observed as a shoulder. [g] No emission observed in any of the solvents at 283 K.

Table III. Excitation Spectral Data for $(OC)_5WL$ and $(OC)_5W$–L–$W(CO)_5$ Complexes in Various Solvents[a]

complex	solvent	excitation max λ_{max}, nm
$(OC)_5W(pyz)W(CO)_5$[b]	CH_2Cl_2	396, 532 (br)
	$CHCl_3$	396, 552 (br)
	C_6H_6	370, 395, 510 (br)
	C_7H_{14}/C_6H_6[c]	394, 548 (br)
$(OC)_5W(bpy)W(CO)_5$	CH_2Cl_2	364, 398
	$CHCl_3$	366, 398
	C_6H_6	364, 400, 432
	C_7H_{14}/C_6H_6[c]	368, 402, 460 (br)
$(OC)_5W(pyz)$[b]	CH_2Cl_2	362, 396
	$CHCl_3$	364, 398
	C_6H_6	364, 396, 434 (w)
	C_7H_{14}/C_6H_6[c]	372, 396, 436 (w)
$(OC)_5W(bpy)$	CH_2Cl_2	366, 398
	$CHCl_3$	366, 398
	C_6H_6	366, 398, 429 (w)
	C_7H_{14}/C_6H_6[c]	372, 402, 454 (w)

[a] Observed in 4×10^{-5}–2×10^{-4} M deoxygenated solutions at 283 K; br = broad, w = weak. Emission monitored at the maximum. [b] Recorded at 298 K. [c] 5:1 (v/v).

and a DMF/CH_2Cl_2 (1:2 v/v) solution are listed in Table IV. Relevant absorption data in these solvents are also shown. Media effects on the MLCT photochemistry of the mononuclear and binuclear complexes have also been investigated. Photolysis leads to the following reactions in all of the solvents studied:[5]

$$(OC)_5WL \xrightarrow[\text{excess L'}]{h\nu} (OC)_5WL' + L \quad (3)$$

$$(OC)_5W\text{–L–}W(CO)_5 \xrightarrow[\text{excess L}]{h\nu} 2(OC)_5WL \quad (4)$$

Photoreaction efficiencies for MLCT excitation of $(OC)_5W(pyz)W(CO)_5$ and $(OC)_5W(bpy)W(CO)_5$ complexes in various solvents are shown in Table V.

Discussion

Electronic Absorption Spectra. Previously it has been determined that the low-lying absorption bands of these mononuclear $(OC)_5WL$ and binuclear $(OC)_5W$–L–$W(CO)_5$ complexes consist of ligand-field (LF) $^1A_1(e^4b_2^2) \rightarrow {}^1E(e^3b_2^2a_1^1)$ and $(W)d\pi \rightarrow \pi^*(L)$ charge-transfer (MLCT) transitions.[4a–f,5] The $(W)d\pi \rightarrow \pi^*(CO)$ transitions in these molecules occur at wavelengths below 300 nm. The low-energy assignments are supported by the solvent effects depicted by data in Figure 1 and Table I; the MLCT bands typically exhibit a characteristic negative solvatochromism, whereas the LF transitions are relatively unaffected as the solvent is varied.[4f] These $(OC)_5W$–L–$W(CO)_5$ molecules are centrosymmetric and possess no permanent dipole moment in the ground state. In recognition of this feature, the strong solvent dependence of the MLCT absorptions in these complexes is attributed to changes in the metal–ligand bond polarity between the ground and excited states and, in addition, to specific solvent–solute and induced dipolar interactions.[4c,6l,n]

In very nonpolar solvents the MLCT absorption of the $(OC)_5W$–L–$W(CO)_5$ (L = pyz, bpy) complexes exhibits the structure of two components (see Figure 1 and Table I). This is in accordance with previously reported MCD and resonance Raman measurements of $(OC)_5W(pyz)W(CO)_5$ indicating that the low-energy absorption band envelope comprises *y*- and *z*-polarized orbitally allowed MLCT transitions that originate from the metal $d(b_{1g})$ and $d(b_{2g})$ orbitals, respectively.[4c] In this molecule the pyrazine ring is defined to lie in the *yz* plane, and the equatorial carbonyl groups are at 45° to the pyrazine plane, yielding an overall D_{2h} symmetry. The *z*-polarized MLCT transition is at lowest energy and is the most solvent sensitive. Henceforth, these two transitions will be referred to as the *y*- and *z*-MLCT components. Similarly, dual MLCT components have also been recorded in MCD, resonance Raman, electronic absorption, and luminescence spectra of $M(CO)_4(\alpha,\alpha'\text{-diimine})$ (M = Cr, Mo, W) complexes.[13]

The LF $^1A_1 \rightarrow {}^1E$ absorptions of each of the binuclear complexes are observed to be relatively unmoved from their corresponding mononuclear derivatives. In contrast the MLCT transitions may be substantially affected on binucleation; these shifts have previously been related to the ligand π^*-acceptor orbital energies.[5] When L = pyz, the MLCT band is substantially red-shifted as the ligand binucleates and forms the bridged dimer, indicating considerable lowering of the energy of the pyz π^*-acceptor orbital. We also note strong solvent effects on the low-lying MLCT absorption band in this ligand-bridged $(OC)_5W(pyz)W(CO)_5$ complex. When L = bpy, the ligand π^*-acceptor orbital is stabilized to a lesser extent on forming the

(13) (a) Staal, L. H.; Stufkens, D. J.; Oskam, A. *Inorg. Chim. Acta* **1978**, *26*, 255. (b) Balk, R. W.; Stufkens, D. J.; Oskam, A. *Inorg. Chim. Acta* **1978**, *28*, 133. (c) Staal, L. H.; Terpstra, A.; Stufkens, D. J. *Inorg. Chim. Acta* **1979**, *34*, 97. (d) Balk, R. W.; Stufkens, D. J.; Oskam, A. *Inorg. Chim. Acta* **1979**, *34*, 267. (e) Balk, R. W.; Snoeck, T.; Stufkens, D. J.; Oskam, A. *Inorg. Chem.* **1980**, *19*, 3015. (f) Manuta, D. M.; Lees, A. J. *Inorg. Chem.* **1983**, *22*, 572. (g) Balk, R. W.; Stufkens, D. J.; Oskam, A. *J. Mol. Struct.* **1980**, *60*, 387. (h) Servaas, P. C.; van Dijk, H. K.; Snoeck, T. L.; Stufkens, D. J.; Oskam, A. *Inorg. Chem.* **1985**, *24*, 4494. (i) Manuta, D. M.; Lees, A. J. *Inorg. Chem.* **1986**, *25*, 1354.

Table IV. Redox Potentials and Electronic Absorption Data of Free Ligands (L) and $(OC)_5WL$ and $(OC)_5W-L-W(CO)_5$ Complexes in Various Solvents at 298 K[a]

complex	solvent[b]	E_{ox}		E_{red}: (0/−), (−/2−), (2−/3−)	λ_{max}, nm: LF	MLCT
$(OC)_5W(pyz)W(CO)_5$	CH_2Cl_2	+1.26 (i)		−1.21, >−2.30	395	521
	DMF/CH_2Cl_2	+1.26 (i)	+1.14 (i)	−0.94, −1.45	394	484
	DMF	+1.16 (i)	+1.00 (i)	−0.84, −1.34, −2.09 (i)	395	446
$(OC)_5W(bpy)W(CO)_5$	CH_2Cl_2		+1.09 (i)	−1.30, −1.80	402	431
	DMF/CH_2Cl_2	+1.32 (i)	+1.12 (i)	−1.20, −1.47, −1.90 (i)	399	426[c]
	DMF		+1.07 (i)	−1.13, −1.42, −1.85	398	424[c]
$(OC)_5W(bpa)W(CO)_5$	CH_2Cl_2		+1.16 (i)	>−2.30	379	335
	DMF/CH_2Cl_2	+1.34 (i)	+1.11 (i)	>−2.30	379	330
	DMF		+1.10 (i)	−1.84, −2.17 (i)	380	310
$(OC)_5W(pyz)$	CH_2Cl_2	+1.25 (i)		−1.70 (i)	398	*d*
	DMF/CH_2Cl_2	+1.26 (i)	+1.10 (i)	−1.44 (i)	394	*d*
	DMF		+1.16 (i)	−0.88, −1.35, −2.08 (i)	390	*d*
$(OC)_5W(bpy)$	CH_2Cl_2		+1.09 (i)	−1.64 (i), −2.04	402	*d*
	DMF/CH_2Cl_2	+1.25 (i)	+0.96 (i)	−1.48 (i), −2.00 (i)	395	*d*
	DMF		+1.09 (i)	−1.27 (i), −1.82	394	*d*
$(OC)_5W(bpa)$	CH_2Cl_2	*e*		*e*	383	*d*
	DMF/CH_2Cl_2	*e*		*e*	379	*d*
	DMF	*e*		*e*	379	*d*
pyz	CH_2Cl_2			>−2.30		
	DMF/CH_2Cl_2			>−2.30		
	DMF			−2.14		
bpy	CH_2Cl_2			−2.10 (i)		
	DMF/CH_2Cl_2			−2.00 (i)		
	DMF			−1.82, −2.24 (i)		
bpa	CH_2Cl_2			>−2.30		
	DMF/CH_2Cl_2			>−2.30		
	DMF			>−2.30		

[a] Analyses performed in $\sim 10^{-3}$ M deoxygenated solutions containing 0.1 M TBAP. All potentials in V vs SCE; scan rate 80 mV/s; scan range +1.40 to −2.30 V; i denotes irreversible process. Liquid-junction correction was neglected. [b] DMF/CH_2Cl_2 is 1:2 (v/v). [c] Observed as a shoulder. [d] Overlaps substantially with LF transition. [e] Value unobtainable due to thermal decomposition of complex.

Table V. Photodissociation Quantum Yields for $(OC)_5W-L-W(CO)_5$ Complexes in Various Solvents[a]

solvent	$(OC)_5W(pyz)W(CO)_5$[b] entering ligand	$10^5\phi_{cr}$ (λ_{ex} = 514 nm)	$(OC)_5W(bpy)W(CO)_5$[c] entering ligand	$10^5\phi_{cr}$ (λ_{ex} = 458 nm)
CH_2Cl_2	pyz	0.6	bpy	5.8
$CHCl_3$	pyz	1.6	bpy	5.5
C_6H_6	pyz	1.3	bpy	4.4
C_7H_{14}/C_6H_6[d]	pyz	1.9	bpy	2.4

[a] Photolysis performed in deoxygenated solutions containing $\sim 10^{-4}$ M complex and 10^{-2} M entering ligand. Quantum yields accurate to ±10%. [b] Recorded at 298 K. [c] Recorded at 283 K. [d] 5:1 (v/v).

ligand-bridged dimer complex, but the solvent dependence of $(OC)_5W(bpy)W(CO)_5$ is still quite significant. When L = bpa, the MLCT absorption band lies at higher energy than the LF transition and the absorption spectra are similar for the mononuclear and binuclear derivatives; thus, there is apparently little effect on the energy position of the bpa π^* orbital as the ligand-bridged complex is formed. Concomitantly, the solvent sensitivity of the MLCT band in $(OC)_5W(bpa)W(CO)_5$ is somewhat less than that observed for the other dimer complexes.

The varying solvatochromism in these $(OC)_5W-L-W(CO)_5$ complexes is interpreted by considering the electronic character of the binucleating ligands, L, and the effects of this on the nature of the resultant MLCT transitions. We note that the ligands here have widely differing basicities; their pK_a values are 0.65 (pyz),[14] 3.03 (bpy),[15] and >7.5 (bpa).[16] The pyz ligand is weakly basic and an excellent π^* acceptor, and it provides a strongly conjugated link between the $(OC)_5W$ moieties in the dimer complex. Thus, the energy of the ligand π^*-acceptor orbital is perturbed greatly on forming the binuclear complex from the mononuclear components. In turn this results in a low-lying MLCT transition, one that involves promotion from the filled metal $d\pi$ orbitals to a relatively pure ligand-localized π^*-acceptor orbital, i.e., $(W)d\pi \rightarrow \pi^*(L)$. In this connection, the previous resonance Raman study of $(OC)_5W(pyz)W(CO)_5$ revealed an enhancement of the pyrazine symmetrical stretching and in-plane bending modes on excitation into the lowest lying absorption band,[4c] consistent with a MLCT transition into the ligand π^* system. The MLCT absorption band is strongly solvent dependent, with its z component being most affected by decreasing bond dipole moments along the z axis in the excited state and by solvent-induced dipole interactions with the ligand π^* orbitals. Although bpy provides a wider bridge between the $(OC)_5W$ fragments, it is still a good π^*-acceptor ligand and the linkage is highly conjugated. Hence, the $(OC)_5W(bpy)W(CO)_5$ complex, for the reasons outlined above, also exhibits a low-lying solvent-sensitive MLCT band. On the other hand, bpa is a much poorer π^*-acceptor ligand and provides an unconjugated bridge between the $(OC)_5W$ groups. In the $(OC)_5W(bpa)W(CO)_5$ complex the MLCT band lies above the LF $^1A_1 \rightarrow {}^1E$ transition and the empty π^*-acceptor orbitals of bpa may be expected to be more heavily mixed with metal $d\pi$ character. Therefore, the MLCT transition in the $(OC)_5W(bpa)W(CO)_5$ complex is likely to involve excitation from filled metal $d\pi$ orbitals to ligand π^* orbitals that are mixed with metal $d\pi$ character, i.e., $(W)d\pi \rightarrow d\pi-\pi^*(L)$. This involves a change in MLCT character to one that produces charge localization primarily along the tungsten–nitrogen bond. Consequently, the z-MLCT transition will exhibit a diminished solvent dependence as variations in bond dipoles along the z axis are reduced and specific solvent and induced dipolar interactions with the ligand π^* system are less influential. The above rationale can also be used to explain the increased solvent sensitivities of the binuclear $(OC)_5W-L-W(CO)_5$ (L = pyz, bpy) complexes over their corresponding mononuclear $(OC)_5WL$ species.

Photophysical Data. The emission results support the MLCT assignments for the lowest energy excited states in the pyz and bpy complexes, whereas the absence of an observable radiative route for the bpa derivatives at room temperature is consistent with a highly photoreactive lowest lying LF $^1A_1 \rightarrow {}^1E$ state.[7,17]

(14) (a) Crutchley, R. J.; Kress, N.; Lever, A. B. P. *J. Am. Chem. Soc.* **1983**, *105*, 1170. (b) Gumbley, S. J.; Lee, T. W. S.; Stewart, R. J. *Heterocycl. Chem.* **1985**, *22*, 1143.
(15) Musgrave, T. R.; Mattson, C. E. *Inorg. Chem.* **1968**, *7*, 1433.
(16) Grandberg, I. I.; Nikitina, S. B.; Kost, A. N.; Faizova, G. K. *Izv. Timiryazevsk. Skh. Akad.* **1968**, *6*, 219.

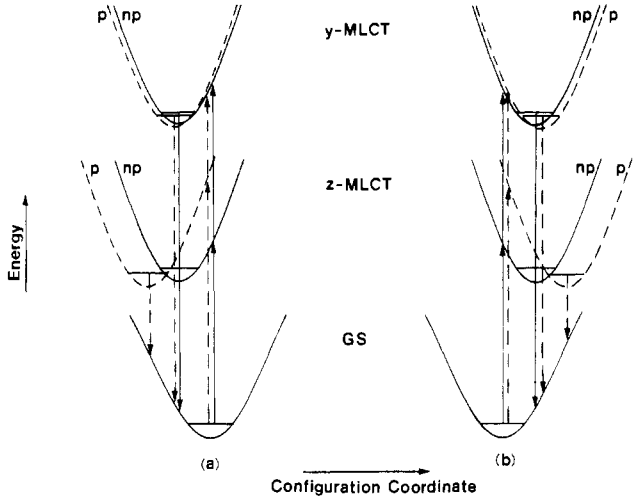

Figure 3. Schematic representation of solvent effects on *y*- and *z*-MLCT excited states relative to the ground state (GS) of $(OC)_5W$-L-$W(CO)_5$ complexes. Schemes illustrate (a) contraction and (b) elongation of the W–L bond in the excited states with respect to the ground state; (—) np and (- - -) p denote nonpolar and polar solvents. Only the radiative processes are shown.

Dual emission features in the spectra of $(OC)_5W(pyz)W(CO)_5$ and $(OC)_5W(bpy)W(CO)_5$ provide further indication of the *y*- and *z*-MLCT excited states. However, the constant lifetime data and the lack of excitation wavelength dependence illustrate that these two MLCT levels are thermally equilibrated at room temperature. Multiple luminescence properties are becoming increasingly recognized for transition-metal complexes,[18] and known organometallic examples include *fac*-$[SRe(CO)_4L]^+$ (S = CH_3CN, PhCN, pyridine, piperidine; L = 1,10-phenanthroline, 2,2′-biquinoline)[19] and *fac*-$XRe(CO)_3L_2$ (X = Cl, Br, I; L = pyridine or a pyridine derivative)[20] complexes, which exhibit intraligand (π–π^* or n–π^*) and Re → π^*(L) CT emissions at 77 K. Recently, dual emissions from thermally equilibrated MLCT states have also been observed from $M(CO)_4(\alpha,\alpha'$-diimine) (M = Cr, Mo, W) complexes in room-temperature solution.[13f,h,i]

As noted in absorption, the emission results illustrate that the lowest energy *z*-MLCT transition exhibits the most solvent sensitivity and the *y*-MLCT band is comparatively less affected.

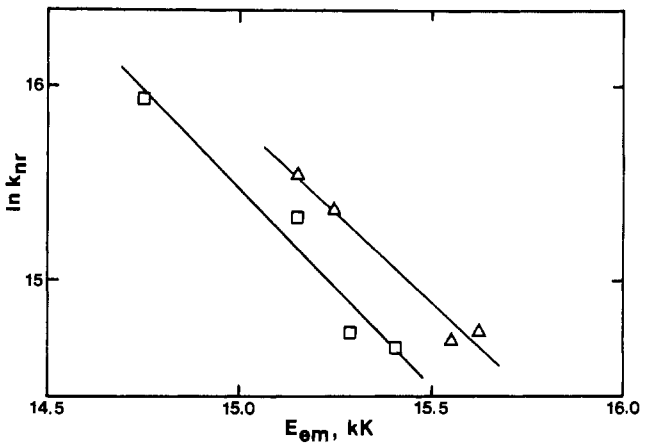

Figure 4. Plot of ln k_{nr} vs E_{em} for (△) $(OC)_5W(bpy)$ and (□) $(OC)_5W(bpy)W(CO)_5$ complexes in various solvents.

Significantly, the solvent dependence of the MLCT emission is in the direction opposite to that observed in the absorption spectra. These seemingly contradictory solvent effects may be interpreted on an excited-state distortion scheme that qualitatively represents the equilibrium geometry and energy of the *y*- and *z*-MLCT excited states relative to the ground state for nonpolar (np) and polar (p) environments (see Figure 3). Schemes a and b both represent possible excited-state distortions that give rise to absorption and emission spectra exhibiting solvent shifts in the opposite direction. These representations also depict the increased solvent sensitivity of the *z*-MLCT transition in comparison to that of the *y*-MLCT component. Realizing that on MLCT excitation the metal is formally oxidized and the ligand reduced, we have chosen to express the nuclear coordinate in these molecules as the average equilibrium geometry of the W–L bond. When considering these schemes, we favor scheme a, involving a contraction of the W–L bond in the MLCT excited state, as this is in accordance with both the electrostatic argument above and the lack of photosubstitution chemistry known for these MLCT excited states.[4f] In this vein, recent calculations of $W(CO)_5$(N-donor) complexes from a time-dependent theoretical treatment of emission and preresonance Raman spectra have illustrated that the largest LF excited-state distortions occur along the molecular axis containing the W–N bond. Specifically, for $W(CO)_5$(py) (py = pyridine) the W–N bond has been estimated to be lengthened by 0.18 Å and the W–C bond that is trans to py is lengthened by 0.12 Å. In contrast, the W–C bonds that are cis to py are only lengthened by 0.04 Å.[21] A similar scheme involving contraction of a Re–L bond in the MLCT excited state has also been proposed to account for the solvent dependence of *fac*-$XRe(CO)_3L$ (X = Cl, Br, I; L = Phpy, bpy) complexes.[20b]

Derived photophysical parameters illustrate that by varying solvent it is primarily k_{nr} that is affected (see Table II). Such changes in k_{nr} can be expected to be produced by solvent dynamic behavior, as reorientations of the surrounding dipoles take place in the ground state and MLCT excited states. The emission data of the bpy complexes can be interpreted with the energy gap law,[22] as plots of ln k_{nr} vary linearly with E_{em} (see Figure 4). Here E_{em} is the energy of the emission band maximum. This simple relationship, however, does not exist for the pyz complexes, and apparently specific solvent–solute and induced dipolar interactions play an important role in the excited-state deactivation mechanism. Additionally, in $(OC)_5W(pyz)$ the solvent effects on k_{nr} may be more complicated by the fact that the emitting MLCT state is very nearly isoenergetic with the photoactive LF $^1A_1 \rightarrow {}^1E$ state.

(17) Recently, the first characterized exception to this principle has been observed, with room-temperature ^{3}LF emission detected from a series of $XRe(CO)_4L$ complexes: Glezen, M. M.; Lees, A. J. *J. Am. Chem. Soc.* **1988**, *110*, 3892. The radiative rates of these Re(I) ^{3}LF emissions are in the range 10^6–10^7 s^{-1}, substantially greater than the W(0) examples here.

(18) (a) For a review of literature appearing up to 1980 see: DeArmond, M. K.; Carlin, C. M. *Coord. Chem. Rev.* **1981**, *36*, 325. (b) Halper, W.; DeArmond, M. K. *J. Lumin.* **1972**, *5*, 225. (c) Merrill, J. T.; DeArmond, M. K. *J. Am. Chem. Soc.* **1979**, *101*, 2045. (d) Sullivan, B. P.; Abruna, H.; Finklea, H. O.; Salmon, D. J.; Nagle, J. K.; Meyer, T. J.; Sprintschnik, H. *Chem. Phys. Lett.* **1978**, *58*, 389. (e) Kirk, A. D.; Porter, G. B. *J. Phys. Chem.* **1980**, *84*, 887. (f) Breddels, P. A.; Berdowski, P. A. M.; Blasse, G. *J. Chem. Soc., Faraday Trans. 2* **1982**, *78*, 595. (g) Rader, R. A.; McMillin, D. R.; Buckner, M. T.; Matthews, T. G.; Casadonte, D. J.; Lengel, R. K.; Whittaker, S. B.; Darmon, L. M.; Lytle, F. E. *J. Am. Chem. Soc.* **1981**, *103*, 5906. (h) Kirchhoff, J. R.; Gamache, R. E.; Blaskie, M. W.; Del Paggio, A. A.; Lengel, R. K.; McMillin, D. R. *Inorg. Chem.* **1983**, *22*, 2380. (i) Sexton, D. A.; Ford, P. C.; Magde, D. *J. Phys. Chem.* **1983**, *87*, 197. (j) Martin, M.; Krogh-Jespersen, M.-B.; Hsu, M.; Tewksbury, J.; Laurent, M.; Viswanath, K.; Patterson, H. *Inorg. Chem.* **1983**, *22*, 647. (k) Segers, D. P.; DeArmond, M. K.; Grutsch, P. A.; Kutal, C. *Inorg. Chem.* **1984**, *23*, 2874. (l) Nishizawa, M.; Suzuki, T. M.; Sprouse, S.; Watts, R. J.; Ford, P. C. *Inorg. Chem.* **1984**, *23*, 1837. (m) Belser, P.; von Zelewsky, A.; Juris, A.; Barigelletti, F.; Balzani, V. *Chem. Phys. Lett.* **1984**, *104*, 100. (n) Blakley, R. L.; Myrick, M. L.; DeArmond, M. K. *J. Am. Chem. Soc.* **1986**, *108*, 7843. (o) Casadonte, D. J.; McMillin, D. R. *J. Am. Chem. Soc.* **1987**, *109*, 331.

(19) Fredericks, S. M.; Luong, J. C.; Wrighton, M. S. *J. Am. Chem. Soc.* **1979**, *101*, 7415.

(20) (a) Giordano, P. J.; Fredericks, S. M.; Wrighton, M. S.; Morse, D. L. *J. Am. Chem. Soc.* **1978**, *100*, 2257. (b) Giordano, P. J.; Wrighton, M. S. *J. Am. Chem. Soc.* **1979**, *101*, 2888.

(21) Tutt, L.; Zink, J. I. *J. Am. Chem. Soc.* **1986**, *108*, 5830.

(22) (a) Englman, R.; Jortner, J. *J. Mol. Phys.* **1970**, *18*, 145. (b) Freed, K. F.; Jortner, J. *J. Chem. Phys.* **1970**, *52*, 6272. (c) Caspar, J. V.; Meyer, T. J. *J. Am. Chem. Soc.* **1983**, *105*, 5583. (d) Caspar, J. V.; Meyer, T. J. *J. Phys. Chem.* **1983**, *87*, 952. (e) Caspar, J. V.; Sullivan, B. P.; Meyer, T. J. *Inorg. Chem.* **1984**, *23*, 2104. (f) Lumpkin, R. S.; Meyer, T. J. *J. Phys. Chem.* **1986**, *90*, 5307.

Indeed, the photoreactivity of this complex on MLCT excitation has been previously reported to be unusually high.[5]

Excitation results support the observations made in absorption, as illustrated by a solvent dependence of the lowest energy excitation band associated with the MLCT emitting states (see Table III). Excitation maxima in the 360–400-nm region are attributed to higher lying LF states that effectively deactivate to the emitting states.[5]

Electrochemistry. Oxidation potentials (E_{ox}) are very similar in all of the complexes studied, indicating that the HOMO levels are relatively unperturbed on forming the ligand-bridged dimers from their mononuclear components. Furthermore, these oxidation potentials are not significantly solvent dependent, consistent with the electronic absorption assignment of a W(dπ) HOMO level. In several instances two E_{ox} values were obtained; this results from slow electron transfer of adsorbed electroactive species on the electrode surface.[23] All of the E_{ox} processes were observed to be irreversible, indicating that these complexes are not stable on oxidation.

Reduction potentials observed from the free ligands and the metal carbonyl complexes represent ligand-centered one-electron processes of the LUMO levels. The first reduction potentials follow the order L > $(OC)_5WL$ > $(OC)_5W-L-W(CO)_5$ (see Table IV), in accordance with the energy stabilization of the ligand π^*-acceptor orbital, this effect being most pronounced for L = pyz, as rationalized above. Similarly, the $E_{red}(0/-)$ values of $(OC)_5W-L-W(CO)_5$ are ordered bpa > bpy > pyz, reflecting the position of the ligand π^* system in these dimer complexes, concordant with that noted in absorption. The first reduction potential processes were generally observed to be irreversible ($E_{pc} - E_{pa} \gg 0.058/n$ V; E_{pc} = cathodic peak potential, E_{pa} = anodic peak potential, n = number of electrons transferred per molecule) for the mononuclear complexes but were quasi-reversible[24] ($E_{pc} - E_{pa} \approx 0.058/n$ V) or reversible for the one-electron reductions of the binuclear molecules, indicating the relative stabilities of these complexes to reduction.

Solvent influences on the reduction potential data indicate that the complexes are more easily reduced in polar media. This result reflects the energy stabilization of the ligand π^*-acceptor orbitals as the solvent becomes more polar and is consistent with the emission spectral data and the relative energy position of the E_{00} levels represented in Figure 3. A further indication of the Franck–Condon perturbations in these $(OC)_5W-L-W(CO)_5$ complexes can be obtained from a comparison of the redox potential differences, E_p, (see eq 5) and the MLCT energies. For

$$E_p = E_{ox} - E_{red}(0/-) \quad (5)$$

$(OC)_5W(pyz)W(CO)_5$ in CH_2Cl_2, the E_p value (for a one-electron process) is 2.47 eV, close to that of the MLCT absorption maximum of 2.38 eV. However, in DMF/CH_2Cl_2 (1:2 v/v), E_p = 2.20 eV and the MLCT energy is 2.56 eV, and in DMF, E_p = 2.00 eV and the MLCT energy is 2.78 eV. This general trend[25] illustrates that as the solvent becomes more polar, increased energy contributions must be invoked in the Franck–Condon perturbation (see eq 6). In eq 6 E_{od} is the optical absorption energy and χ

$$E_{od} = E_p + \chi \quad (6)$$

consists of contributions to the Franck–Condon energy from intermolecular and intramolecular vibrations.[26] For $(OC)_5W(bpy)W(CO)_5$ and $(OC)_5W(bpa)W(CO)_5$ complexes, the energy term χ becomes much more substantial and the large Franck–Condon energies reflect significant distortion in the MLCT excited states. Twisting about the pyridyl rings can occur in these ligand-bridged complexes, and this may contribute appreciably to the Franck–Condon energy term.

Photochemistry. The primary photoreactions of the $(OC)_5WL$ and $(OC)_5W-L-W(CO)_5$ complexes have been shown to involve W–N bond dissociation from the LF $^1A_1(e^4b_2^2) \rightarrow {}^1E(e^3b_2^2a_1^1)$ excited states.[5] In the present study we have investigated solvent effects on the photoreactivity of the $(OC)_5W(pyz)W(CO)_5$ and $(OC)_5W(bpy)W(CO)_5$ complexes following MLCT excitation. Although the photochemical reaction is the same (eq 4) in each of the solvents studied, there are some media effects on the quantum yields (see Table V). For $(OC)_5W(bpy)W(CO)_5$, the quantum yield (ϕ_{cr}) increases as the solvent becomes more polar. We note that in this complex the MLCT state lies below, but fairly close to, the reactive LF $^1A_1 \rightarrow {}^1E$ state. The ϕ_{cr} results can, therefore, be explained if the photoreactivity is associated entirely with the LF $^1A_1 \rightarrow {}^1E$ state, which is populated via thermal activation from the MLCT levels. As the solution becomes more polar, the energy difference between the LF and MLCT states is reduced and, thus, ϕ_{cr} increases. In the case of $(OC)_5W(pyz)W(CO)_5$, however, the energy gap between the LF and MLCT states is much more substantial and, as previously reported, the photochemistry does not necessarily proceed via the reactive LF $^1A_1 \rightarrow {}^1E$ state.[4f] Indeed, the observed ϕ_{cr} values are quite low and show no obvious correlation with solvent or the position of the MLCT absorption maximum. Instead, we raise a tentative alternative suggestion that the apparent photodissociation may be a consequence of the MLCT excited state undergoing deactivation to a "hot" ground state;[27] thus, it may be more correct to relate the solvent influence on ϕ_{cr} to cage effects in the medium. Presently, we are investigating solvent effects on photoreactivity of a wider range of ligand-bridged metal carbonyl complexes to further explore this possibility.

Summary

A combination of spectroscopic, photochemical, and electrochemical techniques has been used to investigate solvent effects on the excited states and deactivation parameters of binuclear $(OC)_5W-L-W(CO)_5$ complexes and their corresponding mononuclear derivatives. Several important features have been identified:

(a) Ligand-bridged $(OC)_5W-L-W(CO)_5$ complexes exhibit a strong negative solvatochromism associated with the MLCT transitions whereas the LF transitions are relatively unaffected. This solvent dependence arises from specific solvent–solute and induced dipolar interactions in addition to changes in metal–ligand bond polarity during the MLCT transition.

(b) Solvent sensitivity in these complexes is profoundly dependent on the electronic characteristics of the ligand and the extent that the ligand π^* orbitals are mixed with metal dπ character.

(c) The MLCT transition in these binuclear complexes actually comprises two orbitally allowed components although these states are thermally equilibrated at room temperature. The two MLCT transitions have widely differing solvent sensitivities. In a number of complexes large intermolecular Franck–Condon perturbations result from the solvent interaction.

(d) Solvent effects on photophysical and photochemical parameters are predominantly influenced by changes in k_{nr} values. There is some basis for interpreting this via an energy gap law relationship, but specific and induced solvent dipolar interactions must be also invoked in the excited-state degradation mechanism.

Acknowledgment. We thank the donors of the Petroleum Research Fund, administered by the American Chemical Society, for support of this research. M.M.Z. gratefully acknowledges receipt of a South African CSIR Fellowship. We also thank Professor B. McDuffie for his generosity in making the electrochemical equipment freely accessible to us.

Registry No. $(OC)_5W(pyz)W(CO)_5$, 70738-71-5; $(OC)_5W(bpy)W(CO)_5$, 81178-10-1; $(OC)_5W(bpa)W(CO)_5$, 81178-11-2; $(OC)_5W(pyz)$, 65761-19-5; $(OC)_5W(bpy)$, 81178-09-8; $(OC)_5W(bpa)$, 113110-67-1.

(23) Bard, A. J.; Faulkner, L. R. *Electrochemical Methods*; Wiley: New York, 1980.
(24) Mabbott, G. A. *J. Chem. Educ.* **1983**, *60*, 697.
(25) This trend is strictly qualitative because the oxidations in these complexes are irreversible and, therefore, the E_{ox} peak potentials are kinetically controlled. We are grateful to a reviewer for pointing this out.
(26) (a) Curtis, J. C.; Sullivan, B. P.; Meyer, T. J. *Inorg. Chem.* **1983**, *22*, 224. (b) Dodsworth, E. S.; Lever, A. B. P. *Chem. Phys. Lett.* **1985**, *19*, 61.
(27) Calvert, J. G.; Pitts, J. N. *Photochemistry*; Wiley-Interscience: New York, 1966; p 646.